Monthly Notices of the ROYAL ASTRONOMICAL SOCIETY
MNRAS **454,** 946–951 (2015) doi:10.1093/mnras/stv2045

MOA-2010-BLG-353Lb: a possible Saturn revealed

N. J. Rattenbury,[1⋆†] D. P. Bennett,[2†] T. Sumi,[3†] N. Koshimoto,[3†] I. A. Bond,[4†] A. Udalski,[5,‡] F. Abe,[6†] A. Bhattacharya,[2†] M. Freeman,[7†] A. Fukui,[8†] Y. Itow,[6†] M. C. A. Li,[1†] C. H. Ling,[4†] K. Masuda,[6†] Y. Matsubara,[6†] Y. Muraki,[6†] K. Ohnishi,[9†] To. Saito,[10†] A. Sharan,[1†] D. J. Sullivan,[11†] D. Suzuki,[2†] P. J. Tristram,[12†] S. Kozłowski,[5,‡] P. Mróz,[5,‡] P. Pietrukowicz,[5,‡] G. Pietrzyński,[5,13,‡] R. Poleski,[5,14,‡] D. Skowron,[5,‡] J. Skowron,[5,‡] I. Soszyński,[5,‡] M. K. Szymański,[5,‡] K. Ulaczyk[5,‡] and Ł. Wyrzykowski[5,‡]

[1]*Department of Physics, University of Auckland, Private Bag 92019, Auckland, New Zealand*
[2]*Department of Physics, University of Notre Dame, Notre Dame, IN 46556, USA*
[3]*Department of Earth and Space Science, Graduate School of Science, Osaka University, 1-1 Machikaneyama, Toyonaka, Osaka 560-0043, Japan*
[4]*Institute of Natural and Mathematical Sciences, Massey University, Private Bag 102-904, North Shore Mail Centre, Auckland, New Zealand*
[5]*Warsaw University Observatory, Al. Ujazdowskie 4, PL-00-478 Warszawa, Poland*
[6]*Solar-Terrestrial Environment Laboratory, Nagoya University, Nagoya 464-8601, Japan*
[7]*School of Physics, The University of New South Wales, Sydney, NSW 2052, Australia*
[8]*Okayama Astrophysical Observatory, National Astronomical Observatory, 3037-5 Honjo, Kamogata, Asakuchi, Okayama 719-0232, Japan*
[9]*Nagano National College of Technology, Nagano 381-8550, Japan*
[10]*Tokyo Metropolitan College of Industrial Technology, Tokyo 116-8523, Japan*
[11]*School of Chemical and Physical Sciences, Victoria University of Wellington, P.O. Box 600, Wellington 6140, New Zealand*
[12]*Mt John Observatory, PO Box 56, Lake Tekapo 8770, New Zealand*
[13]*Departamento de Astronomia, Universidad de Concepción, Casilla 160-C, Concepción, Chile*
[14]*Department of Astronomy, The Ohio State University, 140 West 18th Avenue, Columbus, OH 43210,USA*

Accepted 2015 September 1. Received 2015 August 28; in original form 2015 May 26

ABSTRACT

We report the discovery of a possible planet in microlensing event MOA-2010-BLG-353. This event was only recognized as having a planetary signal after the microlensing event had finished, and following a systematic analysis of all archival data for binary lens microlensing events collected to date. Data for event MOA-2010-BLG-353 were only recorded by the high-cadence observations of the OGLE and MOA survey groups. If we make the assumptions that the probability of the lens star hosting a planet of the measured mass ratio is independent of the lens star mass or distance, and that the source star is in the Galactic bulge, a probability density analysis indicates the planetary system comprises a $0.9^{+1.6}_{-0.53}$ $M_{\rm Saturn}$ mass planet orbiting a $0.18^{+0.32}_{-0.11}$ $M_\odot$ red dwarf star, $6.43^{+1.09}_{-1.15}$ kpc away. The projected separation of the planet from the host star is $1.72^{+0.56}_{-0.48}$ au. Under the additional assumption that the source is on the far side of the Galactic bulge, the probability density analysis favours a lens system comprising a slightly lighter planet.

Key words: gravitational lensing: micro – planets and satellites: detection – stars: individual: MOA-2010-BLG-353.

1 INTRODUCTION

As a planet-detection technique, microlensing is unique in that the peak sensitivity of microlensing to planets falls beyond the host star's snow line. The snow line is defined as the radius in the mid-plane of the protoplanetary disc where the temperature is below the sublimation temperature for water. Crossing the snow line, the density of solid material increases by a factor of a few (Gaudi

⋆ E-mail: n.rattenbury@auckland.ac.nz
† Microlensing Observations in Astrophysics (MOA) Collaboration.
‡ Optical Gravitational Lensing Experiment (OGLE) Group.

2012). Understanding the population of planets that form at or near the snow line is important for the core-accretion theory of planet formation (Ida & Lin 2005). Microlensing searches have discovered cold planets orbiting their host stars (see e.g. Sumi et al. 2010; Gaudi 2012) and has also provided evidence for a large population of free-floating planets – planets without a host star or at least separated by a very large distance from a potential host (Sumi et al. 2011).

Three survey groups now routinely monitor dense stellar fields, looking for microlensing events. These groups and their operations are briefly described below.

The Microlensing Observations in Astrophysics collaboration (MOA; Bond et al. 2001; Sumi et al. 2003) uses the 1.8-m MOA-II telescope at the Mount John University Observatory, Tekapo, New Zealand. The MOA-cam3 camera (Sako et al. 2008) mounted on the MOA-II telescope has a 2.2 deg^2 field of view and is able to observe 50 deg^2 of the Galactic bulge every hour.

The Optical Gravitational Lensing Experiment (OGLE; Udalski, Szymański & Szymański 2015) observe crowded stellar fields using the 1.3-m Warsaw telescope at Las Campanas, Chile. The fourth phase of the OGLE project – OGLE-IV – is currently in operation and monitors over 3000° of the sky. Both the MOA and OGLE survey operations include high-cadence observations (<60 min) for a subset of their fields. Such high-cadence observations led to the discovery of the population of free-floating planets mentioned above and reported by Sumi et al. (2011).

The OGLE survey detects ∼2000 microlensing events every year and the MOA collaboration detects ∼600 events per year. Most of the MOA detections have an OGLE counterpart and the longitudinal separation of Las Campanas and Tekapo means that these events can be well sampled in time by these two survey groups. Both the MOA and OGLE groups issue real-time alerts as new events are discovered.

The Korean Microlensing Network (KMTNet; Park et al. 2012) of three wide field-of-view telescopes located in South Africa, Australia and Chile has also recently started survey operations.

During each year's microlensing 'season' – during the Southern hemisphere winter – microlensing event data are monitored for evidence of a deviation from that expected assuming a single mass is acting as the gravitational lens. Such deviations are found in real time by human observers, and by the expert system ARTEMiS (Dominik et al. 2008, 2010) and the community alerted to the presence of an anomaly that may be owing to a second mass – possibly a planet – in the lens system. Preliminary models are circulated, including those generated automatically by the RTModel system (Bozza 2010; Bozza et al. 2012).[1] In response to anomaly alerts, one or more follow-up collaborations proceed to invest their observational resources to monitor events of particular interest. The follow-up groups, which include μFUN (Gould et al. 2010), PLANET (Albrow et al. 1998), RoboNet (Tsapras et al. 2009) and MiNDSTEp (Dominik et al. 2010) monitor anomalous events as intensely as deemed necessary. These data, combined with the survey data, are used to constrain models of the lens system which could be found to include one or more planets. To date, 28 microlensing planets have been found by microlensing, and the reader is directed to the NASA Exoplanet Archive[2] for details.

Follow-up data were obtained for most microlensing events which showed evidence of a planet or planets. In contrast, some planets have been discovered using survey data alone, e.g. events MOA-2007-BLG-197 (Bennett et al. 2008) and MOA-2008-BLG-379 (Suzuki et al. 2014). While follow-up data were collected for event MOA-2011-BLG-293, the survey data alone were sufficient to characterize the planetary system (Yee et al. 2012). The planet found in event MOA-2011-BLG-322 was found using survey data from the MOA and OGLE groups and the Wise Observatory (Shvartzvald et al. 2014). This present work reports another planet found using microlensing survey data alone. That the data contained a planet anomaly was only discovered after the event, once a systematic search over the binary lens parameter space was made for all archival binary lens microlensing data light curves.

In this paper, we present the analysis of microlensing event MOA-2010-BLG-353. In Sections 2 and 3, we describe the data and their treatment, respectively. The results of modelling the observed light-curve data with a binary lens model are presented in Section 4. An analysis of the background source star is given in Section 5. The planet parameters estimated from a probability density analysis is presented in Section 6; and Section 7 comprises our discussion and conclusion.

2 OBSERVATIONS

Microlensing event MOA-2010-BLG-353 was discovered at (RA, Dec.) = ($18^{\rm h}05^{\rm m}12\overset{\rm s}{.}94$, $-27^\circ17'35\overset{''}{.}64$) and an alert was issued by the MOA collaboration on 2010 July 28. The MOA collaboration observed the field in which MOA-2010-BLG-353 was discovered with a median cadence of 20 min over the course of the event. The MOA observations were made in the custom MOA-red filter, which has a passband corresponding to the sum of the standard I and V filters.

During the period between 2009 May and 2011 May, the OGLE survey team were not issuing alerts to the community as it was upgrading both their camera and Early Warning System software (Udalski 2003). However, the OGLE team did record the I-band data for this event, with a median cadence of 60 min, using the OGLE-IV camera (Udalski et al. 2015).

3 DATA REDUCTION

The images obtained by the MOA telescope were reduced using the difference imaging pipeline of Bond et al. (2001). When analysing a crowded stellar field using difference imaging, a neighbouring star, of a different colour to the target star, can affect the photometry of the target star through the differential refraction effect of the atmosphere. The degree to which the source star's photometry is affected depends on the amplitude and direction of the differential refraction. In addition to discarding extreme outliers, the MOA data were corrected for differential refraction. The final MOA light curve comprised 9130 data points.

The OGLE data set for this event comprises 3248 I-band observations, generated from the OGLE difference imaging analysis pipeline (Udalski 2003). It was not necessary to apply a correction for differential refraction to the OGLE data.

4 BINARY LENS MODELLING

An initial best-fitting binary lens model to the observational data was found from a large-scale grid search over the basic binary lens parameter space. Initial values were found for the mass ratio, $q = M_{\rm p}/M_{\rm L}$, where $M_{\rm p}$ and $M_{\rm L}$ are planet and host lens masses, respectively, the binary lens separation, s, in units of the Einstein

[1] www.fisica.unisa.it/GravitationAstrophysics/RTModel/2014/RTModel.htm

[2] http://exoplanetarchive.ipac.caltech.edu/docs/intro.html#ack

Table 1. Best-fitting binary lens model parameters for planetary microlensing event MOA-2010-BLG-353. Each quoted error is the average of the upper and lower errors determined from the corresponding MCMC parameter state distribution.

Parameter	Value
t_0	5381.24 ± 0.06 HJD $-$ 2450000
t_E	11.3 ± 0.7 d
u_0	$-0.79 \pm 0.08 R_E$
q	$(1.4 \pm 0.4) \times 10^{-3}$
s	$1.45 \pm 0.06\ R_E$
α	4.17 ± 0.02 rad
ρ	$(2.1 \pm 0.9) \times 10^{-2}$

ring radius, the source star track orientation angle α, the minimum impact parameter u_0, the Einstein radius crossing time t_E, the epoch t_0 corresponding to the source star being positioned at u_0 and the relative angular source star radius $\rho = \theta_\star/\theta_E$, where $\theta_\star$ and θ_E are the angular sizes of the source star and Einstein ring radii, respectively.

Starting from the initial best-fitting binary lens solution found from the grid search, we refined the solution using a variant of the image-centred ray-shooting method of Bennett (2010).

We used a linear limb-darkening profile for the source star and chose limb-darkening coefficients based on an estimate of the source star's ($V-I$) colour. This ($V-I$) colour estimate is model dependent. For this reason, we iterated the steps of finding the best-fitting binary lens model using our MCMC algorithm, deriving the corresponding ($V-I$) colour for the source and therefrom the source star limb-darkening coefficients, until the values of the limb-darkening coefficients ceased to change. The details of how we estimated the source colour are presented in Section 5, along with the limb-darkening coefficients used in the final model for this event.

The motion of the Earth in its orbit around the Sun can impart a parallax signal for some microlensing events (Gould 1992; Alcock et al. 1995). This additional effect is generally a desirable one – allowing a more accurate estimate of the lens star mass and distance, and thereby a more accurate estimate of the absolute values of the mass and orbital radius of planetary lens components. Parallax is more likely to be seen in microlensing events with large values of t_E. This event has $t_E \simeq 11$ d, and is therefore a priori unlikely to show any parallax signal. Despite this, we attempted to include microlensing parallax in our models. Not unsurprisingly, we were unable to detect any parallax signal for this event.

The best-fitting binary lens model has the following parameters for the binary lens mass ratio and binary lens separation: $q = (1.4 \pm 0.4) \times 10^{-3}$ and $s = (1.45 \pm 0.06)$. The Einstein ring radius crossing time is $t_E = (11.3 \pm 0.7)$ d. Table 1 lists these and the other parameters in the best-fitting model. The light-curve data during the microlensing event MOA-2010-BLG-353, along with the best-fitting light curve, is shown in Figs 1 and 2. The critical and caustic curves and source star track are shown in Fig. 3.

The best-fitting planetary microlensing model is systematically above the OGLE data points at $t \simeq 5378$. To test whether this discrepancy has any significant effect on our final results, we forced the model to be consistent with the majority of these OGLE data. The parameters of this forced model are consistent with the parameters listed in Table 1. We ascribe the discrepancy to simple statistical fluctuations or to some unrecognized systematics. We conclude therefore that the failure of the best-fitting model to fit the OGLE data at $t \simeq 5378$ does not significantly alter our final results.

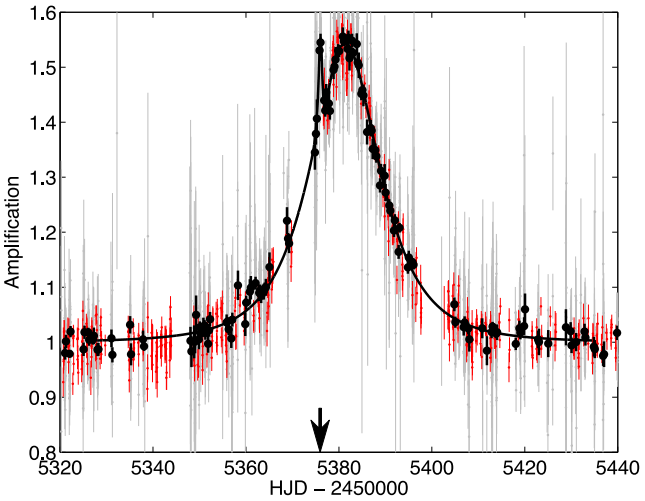

Figure 1. Observed data from the MOA (grey) and OGLE (red) microlensing survey groups for event MOA-2010-BLG-353. Binned MOA data points are shown as black points. The best-fitting binary lens model is also shown (black line). The parameters for this model are given in Table 1. The epoch when the MOA collaboration issued an alert for this event is indicated with a black arrow.

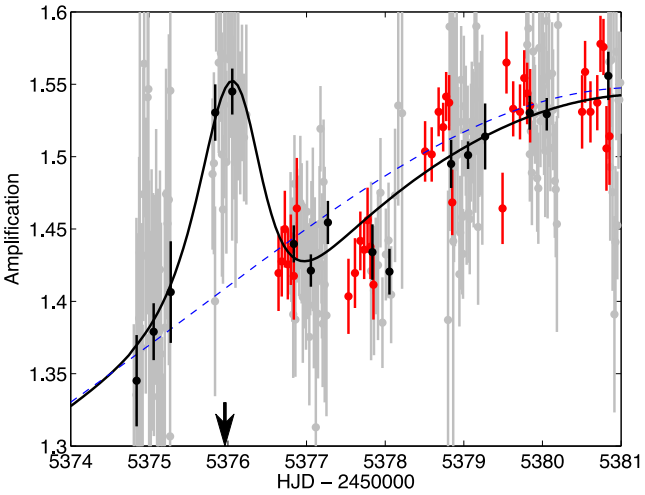

Figure 2. This is a close-up view of the light curve for MOA-2010-BLG-353 as shown in Fig. 1, highlighting the planetary perturbation. The single lens, finite source star model is shown with a dashed blue line.

We also investigated alternatives to the planetary microlensing model for explaining the anomaly at $t \simeq 5376$. We attempted to fit a binary source model to the data (Gaudi 1998) but we were unable to find a superior fit to the data. Similarly, we analysed the baseline data of this event for signs of intrinsic variability in the source. Our tests indicated that the baseline data are randomly ordered.

5 SOURCE STAR

Characterizing the source star in a microlensing event leads to an estimate of the angular size of the Einstein ring in the lens plane, θ_E. This in turn allows tighter constraints to be placed on the binary lens masses and lens separation, see e.g. Suzuki et al. (2014). The value of $\rho = \theta_\star/\theta_E$ is provided by the best-fitting model to the observed light curve, and an estimate of $\theta_\star$ may be made from known relations

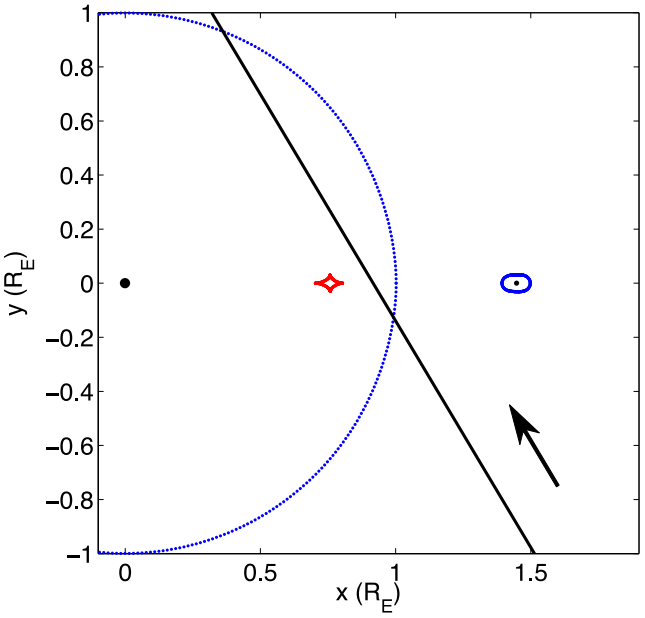

Figure 3. The critical (blue) and caustic (red) curves corresponding to the best-fitting model for planetary microlensing event MOA-2010-BLG-353. The source star track is also shown (black), and the direction of the source star is indicated with an arrow.

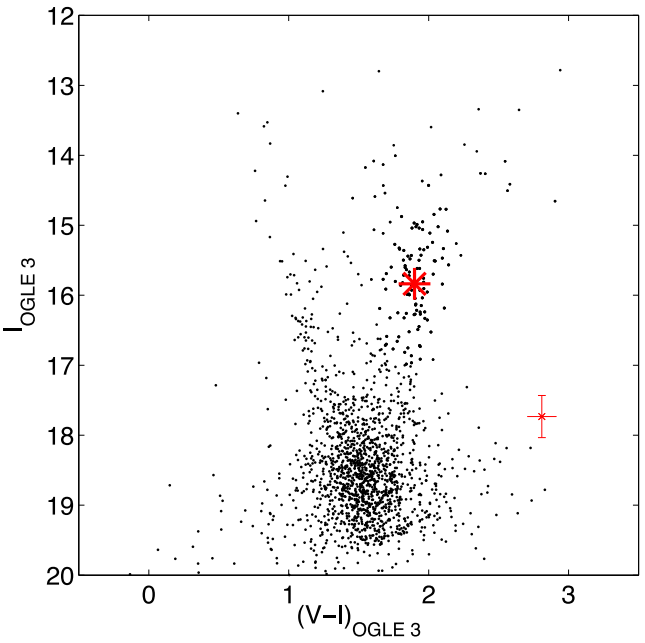

Figure 4. Colour–magnitude diagram of the OGLE-III field stars for event MOA-2010-BLG-353. The centre of the red clump is indicated (asterisk) as is the location of the source star.

between optical colour and stellar radius. Determining the source star's optical colour therefore leads to our desired estimate of $\theta_{\rm E}$.

The first step in determining the source star's optical colour was to cross-match MOA field stars in the 2 arcmin region surrounding the coordinates of event MOA-2010-BLG-353, with stars in the calibrated OGLE-III catalogue (Udalski et al. 2008). This led to a colour–colour relationship between the instrumental MOA and OGLE-III colours, $(R_{\rm MOA} - I_{\rm OGLE3})$ and the calibrated OGLE-III colour $(V - I)_{\rm OGLE3}$. We similarly cross-matched MOA field stars with OGLE-IV field stars and found the relationship between $(R_{\rm MOA} - I_{\rm OGLE4})$ and $(V - I)_{\rm OGLE4}$. Using the instrumental source colour, $(R_{\rm MOA} - I_{\rm OGLE4})_{\rm S}$, obtained from the best-fitting model, we used this last relation to estimate the instrumental source colour in the OGLE-IV photometric scale, $(V - I)_{\rm OGLE4,\,S}$. Cross-matching OGLE-III and OGLE-IV field stars, we fitted a straight line of the form $(I_{\rm OGLE3} - I_{\rm OGLE4}) = a(V - I)_{\rm OGLE4} + b$. This relation, allows us to obtain $(R_{\rm MOA} - I_{\rm OGLE3})_{\rm S}$ and with our first colour–colour relationship, find an estimate of the source colour $(V - I)_{\rm OGLE3,\,S}$ and magnitude $I_{\rm OGLE3,\,S}$:[3]

$$I_{\rm S} = 17.73 \pm 0.3$$
$$(V - I)_{\rm S} = 2.81 \pm 0.1,$$

where the errors above include – in quadrature – errors arising from the light-curve modelling, and the uncertainties arising from the colour–colour relationships. A colour–magnitude diagram of the OGLE-III field stars is shown in Fig. 4.

We make the usual assumption that the source is located in the Galactic bulge and is therefore subject to the same reddening and extinction as bulge red clump giant stars. Red clump giant stars have tightly defined magnitudes and colours, and are therefore often used as standard candles for Galactic structure studies (Cao et al. 2013). Using a colour–magnitude diagram of the OGLE-III field stars for event MOA-2010-BLG-353, we found the centroid of the red clump:

$$I_{\rm RCG} = 15.62 \pm 0.05$$
$$(V - I)_{\rm RCG} = 1.89 \pm 0.01.$$

The intrinsic luminosity parameters of the Galactic bulge red clump are estimated in Nataf et al. (2013) to be $I_{\rm RCG,\,0} = 14.44 \pm 0.04$ with the colour of the red clump being centred at $(V - I)_{\rm RCG,\,0} = 1.06$ with dispersion 0.121.

Comparing the observed RCG centroid colour and magnitude with these RCG intrinsic values, we find the extinction and reddening towards MOA-2010-BLG-353 to be $(A_{\rm I}, E(V-I)) = (1.18, 0.83) \pm (0.07, 0.12)$. The intrinsic source colour and magnitude are therefore $(I, V - I)_{\rm S,\,0} = (16.55, 1.98) \pm (0.31, 0.16)$. The source magnitude and colour is consistent with a K5 subgiant in the Galactic bulge. From table 5 of Bessell et al. (1998), we estimate the surface temperature of a giant star with $(V - I) = 1.98$ to be $T_{\rm eff} \simeq 3750$ K. This surface temperature corresponds to linear limb-darkening coefficients in the I and $R_{\rm MOA}$ bands of $(c_{\rm I}, c_{R_{\rm MOA}}) = (0.5937, 0.6414)$ where $c_{R_{\rm MOA}}$ is computed as the average of the limb-darkening coefficients in the R and I bands. The limb-darkening coefficients differ only very slightly if we assume a subgiant source star with a cooler $T_{\rm eff} = 3500$ K.

With the intrinsic source colour in hand, we can use the relationship between optical colour and brightness radius in Kervella & Fouqué (2008) to estimate the source star's angular radius: $\theta_\star = 3.97 \pm 0.89$ μas. Combined with the model value of the source star angular radius relative to the angular Einstein ring radius, $\rho = \theta_\star/\theta_{\rm E} = (2.12 \pm 0.89) \times 10^{-2}$, we derive a value of angular Einstein ring radius, $\theta_{\rm E} = 0.187 \pm 0.089$ mas.

6 LENS SYSTEM PARAMETER ESTIMATION

Without a measurement of microlensing parallax in event MOA-2010-BLG-353, we have to appeal to statistical arguments in order

[3] As the OGLE-III colours are calibrated, we will delete the OGLE-III subscript.

to provide an estimate of the lens mass and distance. We followed a similar analysis to that of Beaulieu et al. (2006) to generate probability densities for the lens mass and lens and source distances.

The modelled t_E and the calculated Einstein ring radius θ_E are related to the lens and source distances from the observer – D_L and D_S, respectively – and the lens mass M_L, via the relation $\theta_E^2 = \kappa M_L (1/D_L - 1/D_S)$ where $\kappa = 8.14$ mas/M$_\odot$. We find the lens system to comprise a star with mass $0.18^{+0.32}_{-0.11}$ M$_\odot$ with a planet of mass $0.9^{+1.6}_{-0.53}$ $M_{\rm Saturn}$. The projected separation between the host star and the planet is $1.72^{+0.56}_{-0.48}$ au. The distance to the lens system is $6.43^{+1.09}_{-1.15}$ kpc.

The probability density analysis was rerun, this time leaving out the constraints imposed by our estimate of θ_E. The results are essentially the same as those found above. The planet has a mass of $1.03^{+1.73}_{-0.65}$ $M_{\rm Saturn}$ and orbits a $0.21^{+0.35}_{-0.13}$ M$_\odot$ star $6.21^{+1.19}_{-1.44}$ kpc distant. The projected orbital radius is now $1.85^{+0.79}_{-0.65}$ au. The planet parameters estimated from our probability density analyses are essentially independent of our characterization of the source star.

It is important to note that the lens system parameters found from the Bayesean probability density analysis are subject to some important assumptions. The first assumption is that the probability of the planet system comprising a planet with the measured mass ratio is independent of the mass of the host star and the host star's distance. This may not be the case in reality. We also assume that the orientation of the planetary system is random, and that the distribution of planetary radii is uniform. This affects our interpretation of the planet–star separation. If planets at large orbit radii are more common than planets with smaller orbital radii, the separation between host and planet along the line of sight would be much larger than the projected separation.

6.1 A distant source star

One peculiar aspect of event MOA-2010-BLG-353 is the colour of the source star. The very red colour of the source may, in part, be accounted for if the source star was behind the Galactic bulge, at distances greater than the usual assumed value of 8 kpc. For this reason, we reran the likelihood analysis, this time requiring the source star to be located on the far side of the Galactic bulge. We found the range of distances for which a G/K subgiant star would have a colour and magnitude consistent the observed source star, within the quoted errors. In estimating the range of distances for the source, we included the dust extinction profile in the direction of event MOA-2010-BLG-353 from the high-resolution 3D dust extinction map of Schultheis et al. (2014). We found that a K5 subgiant at distances 8.25 kpc $<$ D$_S$ $<$ 9.75 kpc has a colour and magnitude consistent with the source of MOA-2010-BLG-353. When we include this constraint on D_S, the lens system parameters returned by our probability density analysis – including constraints arising from our measurement of θ_E – now correspond to a $0.78^{+1.4}_{-0.43}$ $M_{\rm Saturn}$ planet orbiting a $0.16^{+0.28}_{-0.09}$ M$_\odot$ star at a projected orbital radius of $1.85^{+0.63}_{-0.51}$ au. The lens system is $7.17^{+0.87}_{-1.12}$ kpc distant.

7 DISCUSSION AND CONCLUSION

Microlensing event MOA-2010-BLG-353 has an anomalous signal consistent with a planetary lens system. The best-fitting binary lens model for this event has a binary mass ratio of $q = (1.4 \pm 0.4) \times 10^{-3}$ and the binary lens elements are separated by $s = 1.45 \pm 0.06$ R_E. We were not able to find a binary source model which fits the data better than the best-fitting planetary microlensing model. The variability of the source at the baseline is consistent with random noise.

A measurement of microlensing parallax was not possible for this event and so a well-constrained estimate of the binary lens parameters was not possible.

While a parallax signature was not evident in the data, the finite size of the source star could be modelled. However, the nature of the source star is uncertain. The source appears much redder than the majority of field stars for this event. Given the observed source colour and magnitude, we estimate the source is a K subgiant star in the Galactic bulge. However, the source may be blended with a nearby red star, leading to an incorrect categorisation of the source star. A determination of the source star colour allowed an estimation of the angular radius of the angular Einstein ring radius. The errors on this measurement however, are large, and the θ_E measurement does not serve to constrain a probability density analysis of the binary lens system parameters.

Subject to some important assumptions, the probability density analysis for the lens system parameters suggests that the binary lens system for MOA-2010-BLG-353 is consistent with a $0.9^{+1.6}_{-0.53}$ $M_{\rm Saturn}$ planet orbiting a $0.18^{+0.32}_{-0.11}$ M$_\odot$ M-dwarf, $6.43^{+1.09}_{-1.15}$ kpc away. The projected planet–star distance is $1.72^{+0.56}_{-0.48}$ au. One of these assumptions is that the source star resides in the Galactic bulge, at 8 kpc from our Sun. The very red colour of the source hints at the possibility that the source resides on the far side of the bulge. By constraining the position of the source star to be on the far side of the Galactic bulge, we find that our probability density analysis favours a lens system comprising a $0.78^{+1.4}_{-0.43}$ $M_{\rm Saturn}$ planet orbiting a $0.16^{+0.28}_{-0.09}$ M$_\odot$ star at a projected orbital radius of $1.85^{+0.63}_{-0.51}$ au, with the lens system $7.17^{+0.87}_{-1.12}$ kpc distant.

The planetary signal in MOA-2010-BLG-353 was not identified as such during the microlensing event. It was only during a subsequent systematic analysis of archived light-curve data that MOA-2010-BLG-353 was found to have an anomalous signal, possibly owing to a planet. Without a planetary anomaly alert issued in good time, no observations by the follow-up teams were made of this event. Only MOA and OGLE survey data were recorded for MOA-2010-BLG-353. This discovery re-emphasizes the importance of conducting a systematic parameter search for all events in archival data, as pointed out by Suzuki et al. (2014). It also demonstrates how planets can be found through high cadence microlensing survey operations alone.

The Korean Microlensing Telescope Network epitomizes this new mode of 'survey-only' planetary microlensing. However, we note that an over-reliance on solitary telescope observations, without supporting a system of contemporaneous follow-up observations, may result in missed opportunities. In MOA-2010-BLG-353 we see the planetary anomaly essentially only in the MOA data. In the event of telescope failure, or unfavourable observing conditions, this anomaly would have gone unrecorded.

ACKNOWLEDGEMENTS

NJR is a Royal Society of New Zealand Rutherford Discovery Fellow. AS is a University of Auckland Doctoral Scholar. TS acknowledges financial support from the Japan Society for the Promotion of Science (JSPS) under grant numbers JSPS23103002, JSPS24253004 and JSPS26247023. NK is supported by Grant-in-Aid for JSPS Fellows. The MOA project is supported by JSPS grants JSPS25103508 and JSPS23340064 and by the Royal Society of New Zealand Marsden Grant MAU1104. This research has

made use of the NASA Exoplanet Archive, which is operated by the California Institute of Technology, under contract with the National Aeronautics and Space Administration under the Exoplanet Exploration Program. NJR acknowledges the contribution of NeSI high-performance computing facilities to the results of this research. NZ's national facilities are provided by the NZ eScience Infrastructure and funded jointly by NeSI's collaborator institutions and through the Ministry of Business, Innovation & Employment's Research Infrastructure programme (available at https://www.nesi.org.nz).

REFERENCES

Albrow M. et al., 1998, ApJ, 509, 687
Alcock C. et al., 1995, ApJ, 454, L125
Beaulieu J.-P. et al., 2006, Nature, 439, 437
Bennett D. P., 2010, ApJ, 716, 1408
Bennett D. P. et al., 2008, ApJ, 684, 663
Bessell M. S., Castelli F., Plez B., 1998, A&A, 333, 231
Bond I. A. et al., 2001, MNRAS, 327, 868
Bozza V., 2010, MNRAS, 408, 2188
Bozza V. et al., 2012, MNRAS, 424, 902
Cao L., Mao S., Nataf D., Rattenbury N. J., Gould A., 2013, MNRAS, 434, 595
Dominik M. et al., 2008, Astron. Nachr., 329, 248
Dominik M. et al., 2010, Astron. Nachr., 331, 671
Gaudi B. S., 1998, ApJ, 506, 533
Gaudi B. S., 2012, ARA&A, 50, 411
Gould A., 1992, ApJ, 392, 442
Gould A. et al., 2010, ApJ, 720, 1073
Ida S., Lin D. N. C., 2005, ApJ, 626, 1045
Kervella P., Fouqué P., 2008, A&A, 491, 855
Nataf D. M. et al., 2013, ApJ, 769, 88
Park B.-G. et al., 2012, in Stepp L. M., Gilmozzi R., Hall H. J., eds, Proc. SPIE Conf. Ser. Vol. 8444, Ground-based and Airborne Telescopes IV. SPIE, Bellingham, p. 47
Sako T. et al., 2008, Exp. Astron., 22, 51
Schultheis M. et al., 2014, A&A, 566, A120
Shvartzvald Y. et al., 2014, MNRAS, 439, 604
Sumi T. et al., 2003, ApJ, 591, 204
Sumi T. et al., 2010, ApJ, 710, 1641
Sumi T. et al., 2011, Nature, 473, 349
Suzuki D. et al., 2014, ApJ, 780, 123
Tsapras Y. et al., 2009, Astron. Nachr., 330, 4
Udalski A., 2003, Acta Astron., 53, 291
Udalski A., Szymanski M. K., Soszynski I., Poleski R., 2008, Acta Astron., 58, 69
Udalski A., Szymański M. K., Szymański G., 2015, Acta Astron., 65, 1
Yee J. C. et al., 2012, ApJ, 755, 102

This paper has been typeset from a TEX/LATEX file prepared by the author.